Title
Carvedilol as a potential novel agent for the treatment of Alzheimer's disease

Journal
Neurobiology of Aging, 32(12)

ISSN
0197-4580

Authors
Wang, Jun
Ono, Kenjiro
Dickstein, Dara L
et al.

Publication Date
2011-12-01

DOI
10.1016/j.neurobiolaging.2010.05.004

Peer reviewed

Published in final edited form as:
Neurobiol Aging. 2011 December ; 32(12): 2321.e1–2321.e12. doi:10.1016/j.neurobiolaging.2010.05.004.

Carvedilol as a potential novel agent for the treatment of Alzheimer's disease

Jun Wang[1,2], **Kenjiro Ono**[4], **Dara L. Dickstein**[3], **Isabel Arrieta-Cruz**[1], **Wei Zhao**[1], **Xianjuan Qian**[1], **Ashley Lamparello**[1], **Rakesh Subnani**[1], **Mario Ferruzzi**[5], **Constantine Pavlides**[6], **Lap Ho**[1,2,7], **Patrick R. Hof**[3], **David B. Teplow**[4], and **Giulio M. Pasinetti**[1,2,3,7,*]

[1] Department of Neurology, Mount Sinai School of Medicine, New York, New York 10029

[2] Department of Psychiatry, Mount Sinai School of Medicine, New York, New York 10029

[3] Department of Neuroscience, Mount Sinai School of Medicine, New York, New York 10029

[4] Department of Neurology, David Geffen School of Medicine, Brain Research Institute, and Molecular Biology Institute, University of California, Los Angeles, California 90095

[5] Department of Food Science, Purdue University, West Lafayette, Indiana 47907

[6] The Rockefeller University, New York, New York 10021

[7] Geriatric Research Education and Clinical Center, James J. Peters Veterans Affairs Medical Center, Bronx, New York 10468

Abstract

Oligomeric β-amyloid (Aβ) has recently been linked to synaptic plasticity deficits, which play a major role in progressive cognitive decline in Alzheimer's disease (AD). Here we present evidence that chronic oral administration of carvedilol, a nonselective β-adrenergic receptor blocker, significantly attenuates brain oligomeric Aβ content and cognitive deterioration in two independent AD mouse models. We found that carvedilol treatment significantly improved neuronal transmission, and that this improvement was associated with the maintenance of number of the less stable "learning" thin spines in the brains of AD mice. Our novel observation that carvedilol interferes with the neuropathologic, biochemical and electrophysiological mechanisms underlying cognitive deterioration in AD supports the potential development of carvedilol as a treatment for AD.

Keywords

Oligomeric Aβ; cognitive function; spatial memory; basal neuronal transmission; dendritic spine; synaptic plasticity; bioavailability

[*]Correspondence to: Giulio Maria Pasinetti, M.D., Ph.D., Department of Neurology, The Mount Sinai School of Medicine, 1425 Madison Avenue, Box 1230, New York, NY 10029, Phone: (212) 659-8716, (212) 659-8740, Fax: (212) 876-9042, giulio.pasinetti@mssm.edu.

Conflict of Interest

We declare that there are no competing financial interests in relation to the work described.

Introduction

Alzheimer's disease (AD) is a devastating neurological disorder that imposes a tremendous health burden on society. Currently available palliative medications have not demonstrated significant beneficial effects in AD (Lyketsos et al., 2004) and treat symptoms only.

Growing evidence suggests that cognitive deterioration in AD is directly linked to the accumulation of extracellular soluble oligomeric β-amyloid (Aβ) species, rather than amyloid plaque deposition in the brain (Lambert et al., 1998; Kotilinek et al., 2002; Gylys et al., 2003; Cleary et al., 2005; Klyubin et al., 2005; Lesne S et al., 2006; Shankar et al., 2008). Oligomeric Aβ induces synapse degeneration and synaptic plasticity disruption, which contribute to mechanisms underlying the onset and progression of dementia in AD (Terry et al., 1991; Selkoe, 2002; Walsh et al., 2002; Scheff and Price, 2003; Lacor et al., 2004; Coleman et al., 2004; Jacobsen et al., 2006; Shankar et al., 2007; Shankar et al., 2008). Thus, interference with oligomeric Aβ formation presents a viable preventative and/or therapeutic strategy for AD dementia(Klein, 2002; McLaurin et al., 2006; Seabrook et al., 2007; Zhao et al., 2009).

Carvedilol is a nonselective β-adrenergic receptor blocker, widely prescribed for treating congestive heart failure and hypertension (Packer et al., 1996). Previous structural analysis suggested that carvedilol possesses a specific three-dimensional pharmacophore conformation, associated with the ability to bind Aβ and prevent Aβ from forming oligomeric fibrils (Howlett et al., 1999). A recent study suggested that use of carvedilol is associated with cognitive benefits in AD patients (Rosenberg et al., 2008). In the present study, we explored the potential beneficial role of carvedilol in AD neuropathology and cognitive deterioration in mouse models of AD, in addition to the potential mechanism associated with its beneficial effect.

Materials and Methods

Animals

TgCRND8 transgenic mice carrying a human amyloid precursor protein (APP) containing a familial AD double mutation (Swedish KM670/671NL and Indiana V717F) (Chishti et al., 2001), expressed under the control of a prion promoter, were generated by mating TgCRND8 males with wild type (WT) females (Charles River, Wilmington, MA, USA). The offspring of the WT and heterozygous TgCRND8 were genotyped at 30 days of age. A second, independent AD mouse model (Tg2576 AD transgenic mice) engineered to express APP containing the familial AD Swedish mutation (Hsiao et al., 1996) were purchased from Taconic.

All mice were housed with food and water available *ad libitum*, and maintained on a 12:12-h light/dark cycle with lights on at 07:00 h in a temperature-controlled (20 ± 2 °C) room prior to experimental manipulation. All procedures and protocols were approved by the Mount Sinai School of Medicine's Institutional Animal Care and Use Committee (IACUC) through the Center for Comparative Medicine and Surgery.

Carvedilol treatment

Female TgCRND8 mice were treated with 1.5 mg/kg/day of carvedilol delivered in their drinking water, starting at 8 weeks of age. Using USDA-recommended formulation for converting equivalent drug dosage between species, 1.5 mg/kg/day is equivalent to 7.5 mg per day in human (U.S. Food and Drug Administration: http://www.fda.gov/cber/gdlns/dose.htm). TgCRND8 mice were assigned to two groups: carvedilol treatment and water control groups. Animals had free access to both liquid and

standard chow. Drinking solutions were changed once every week. After 5 months of treatment, mice were sacrificed by decapitation. Brains were harvested as previously described (Wang et al., 2005). Tg2576 mice were treated with the same dose of carvedilol for 7 months, starting at 5 months of age.

Photo-induced cross-linking of unmodified proteins assay (PICUP)

Freshly isolated low molecular weight $A\beta_{1-42}$ (10–20 μM) or $A\beta_{1-40}$ (30–40 μM) peptides were mixed with 1 μl of 1 mM tris (2,2′-bipyridyl)dichlororuthenium(II) (Ru(bpy)) and 1 μl of 20 mM ammonium persulfate (APS) in the presence or absence of equal molar concentration of carvedilol or 10 fold excess of carvedilol. The mixture was irradiated for 1 second, and quenched immediately with 10 μl of Tricine sample buffer (Invitrogen) containing 5% β-mercaptoethanol (Bitan et al., 2001). The reaction was subjected to SDS-PAGE and visualized by silver staining (SilverXpress, Invitrogen).

Circular dichroism spectroscopy (CD)

CD spectra of Aβ:carvedilol mixtures were acquired immediately after sample preparation or following 2, 3, 6, or 7 days of incubation. CD measurements were made by removing a 200 ml aliquot from the reaction mixture, adding the aliquot to a 1 mm path length CD cuvette (Hellma, Forest Hills, NY), and acquiring spectra in a J-810 spectropolarimeter (JASCO, Tokyo, Japan). The CD cuvettes were maintained on ice prior to introduction into the spectrometer. Following temperature equilibration, spectra were recorded at 22°C from ~190–260 nm at 0.2 nm resolution with a scan rate of 100 nm/min. Ten scans were acquired and averaged for each sample. Raw data were manipulated by smoothing and subtraction of buffer spectra according to the manufacturer's instructions.

Electron microscopy (EM)

A 10 μl aliquot of each sample was spotted onto a glow-discharged, carbon-coated Formvar grid (Electron Microscopy Sciences, Hatfield, PA) and incubated for 20 min. The droplet then was displaced with an equal volume of 2.5% (v/v) glutaraldehyde in water and incubated for an additional 5 min. Finally, the peptide was stained with 8 μl of 1% (v/v) filtered (0.2 mm) uranyl acetate in water (Electron Microscopy Sciences, Hatfield, PA). This solution was wicked off and then the grid was air-dried. Samples were examined using a JEOL CX100 transmission electron microscopy.

Bioavailability of Carvedilol

Mouse brain specimens were harvested and carvedilol was extracted from homogenized brain tissue with diethyl ether (3x). Ether fractions were combined and frozen at −80°C for 20 min, after which extracts were filtered, dried under vacuum and resolublized in 400 μL mobile phase prior to analysis by HPLC-MS. Carvedilol separations were performed on a Waters 2695 separations system using an Xterra C18 column (3 μm, 150 × 3.9mm i.d) and resolved using an isocratic mobile phase consisting of solvent ddH_2O:acetonitrile:formic acid (64.9:35:0.1) at a flow rate of 0.7 mL/min. Following separation the column effluent was introduced by positive mode electrospray ionization (ESI) into a Waters ZQ MSD. Mass data (from m/z 150–650) were collected and analyzed using Empower2 software.

Behavioral assessment of cognitive functions by the Morris water maze test and novel object recognition test

Spatial learning memory was assessed by the Morris water maze behavioral test, as previously described (Morris, 1984; Wang et al., 2007). Mice were tested in a 1.25 m circular pool filled with water mixed with non-toxic white paint (Dick Blick Art Materials, IL). In the initial learning phase, mice were exposed to daily training sessions over 7

consecutive days which were designed to allow the animals to learn to escape from the water by using the spatial cues provided to localize and then climb onto a hidden/submerged (1.5 cm below-water surface) escape platform (14×14 cm) in a restricted region of the pool. Spatial memory is assessed by recording the latency time for the animal to escape from the water onto the submerged escape platform as a function of the number of learning trials during the learning phase. Twenty-four hours after the learning phase, mice were subjected to a 45 second probe trial wherein the escape platform was removed. Spatial memory retention is reflected by the increasing proportion of time animals spent within the "target" quadrant of the pool that previously contained the hidden escape platform. Water maze activity during training and probe trials was monitored with the San Diego Instrument Poly-Track video tracking system (San Diego, CA).

Novel object recognition memory tests were performed as described by Bevins and Besheers (Bevins and Besheer, 2006). During the first consecutive 5 days of the object recognition test, animals were exposed for 10 minutes each day to the test environment comprised of a 40 cm squared white box. On the testing day, the mouse was placed into the empty box for one minute and then returned to the home cage. The testing mouse was subsequently subjected to a learning trial in which they were given the opportunity to familiarize themselves with two identical test objects placed in symmetrical location at opposite ends of the box for 10 minutes. One hour (short-term memory testing) or 24 hours (long-term memory testing) after the learning trial, animals were given an object recognition test to assess whether or not they "remember" that they have been exposed to the test object during the learning trial. The object recognition test was conducted by placing each individual mouse into the testing box containing the familiarized "old" object and a novel ("new") object that are located, respectively, at each end of the cage. Each mouse was kept in the cage for 10 minutes, and its behavior during the entire period was recorded by the San Diego Instrument Poly-Track video tracking system (San Diego, CA). The videos were scored, in blind to the treatment schedule, based on the frequency of individual mice to interact with either the familiarized "old" or the novel "new" object. Interaction or no interaction was scored by counting the amount of time spent (in seconds), by the mouse, in contact (nose pointing at and touching the object) with the objects

Assessment of AD-type amyloid neuropathology

Total $A\beta_{1–40}$ or $A\beta_{1–42}$ in the brain were quantified by sandwich ELISA (BioSource, Camarillo, CA), as previously described (Wang et al., 2005). The level of soluble Aβ oligomers was measured by three independent assays: dot blot assay, western blot analysis (McLaurin et al., 2006; Wang et al., 2008), and by ELISA (Wang et al., 2008). Soluble amyloid peptide was extracted in PBS and centrifuged at 78,500 × g for 1 hour at 4 °C, and the supernate was analyzed either by dot blot using A11 antibody specific for oligomeric forms of Aβ or western analysis using the 6E10 (Signet) or A11 antibody. Immunoreactive signals were visualized and quantified. For quantitative oligomeric Aβ analysis, the same sample was applied to a commercially available ELISA kit that specifically detects aggregated beta amyloid using protocols provided by the manufacturer (Invitrogen).

Plaque and spine analysis

Animals were perfused transcardially with 4% paraformaldehyde in phosphate buffer and 0.125% glutaraldehyde. Brain specimens were carefully removed from the skull and postfixed in 4% paraformaldehyde/0.125% glutaraldehyde in phosphate buffer for 6 hours. Fixed brain hemispheres were sectioned on a Vibratome at 50 μm for plaque count and 200 μm for cell loading experiments. Plaque burden was analyzed as previously described (Wang et al., 2005). Briefly, tissue was stained with thioflavin-S and micrograph was taken.

Plaque burden was quantified using Image J software that converts micrograph to binary images for plaque number and plaque area analysis.

For dendritic spine analysis, individual neurons in the fixed frontal cortex were identified by 4,6-diamidino-2-phenylindole (DAPI; Sigma, St. Louis, MO, USA) and injected with 5% Lucifer Yellow (Molecular Probes, Eugene, OR) under a DC current of 3–8 nA for 5–10 minutes or until the dye has filled distal processes and no further loading is observed. Brain sections containing loaded neurons were then mounted in Permafluor mounting medium (Immunotech, Marseille, France) on glass slides. The cells were then traced using a 63X/1.4 N.A. Plan-Apochromat objective on a Zeiss Axiophot microscope equipped with a motorized stage, video camera system, and Neurolucida morphometry software (MBF Bioscience). Individually, Lucifer Yellow-loaded neurons must satisfy the following criteria before it is included in the analysis: (1) lie within layer II/III of the frontal cortex as defined by cytoarchitectural criteria; (2) demonstrate complete filling of dendritic tree; (3) demonstrate intact primary and secondary branches; (4) demonstrate intact tertiary branches (Duan et al., 2002; Duan et al., 2003). Using NeuroExplorer software (MBF Bioscience) total dendritic length, total branch number, number of intersections and the amount of dendritic material per radial distance from the soma, in 30 μm increments (Sholl A and Uttley AM, 2009) were analyzed in order to assess morphological variations. Third and fourth order dendritic segments were used to avoid bias of spines (Duan et al., 2003; Hao et al., 2006; Radley et al., 2006). Dendritic segments, 20–25 μm in length, were imaged on the LSM 410 using a 100X/1.4 N.A. Plan-Apochromat objective with a digital zoom of 5 and an Ar/Kr laser at an excitation wavelength of 488 nm. All confocal stacks were acquired at 512 × 512 pixel resolution with a z-step of 0.1 μm, a pinhole setting of 1 Airy unit and optimal settings for gain and offset. In order for a dendritic segment to be optically imaged it has to satisfy the following criteria: (1) the entire segment has to fall within a depth of 50 μm; (2) segments have to be either parallel or at acute angles to the coronal surface of the section; and (3) segments do not overlap other segments that would obscure visualization of spines.

Confocal stacks were then deconvolved using an iterative blind deconvolution algorithm (AutoDeblur version 8.0.2; Autoquant, Troy, NY). This step is necessary since the image spreads along the Z plane of the raw image limits the precise interpretation of 3D spine morphology. The deconvolution step converts out of focus signal to focused signal and results in images where dendritic diameters and spine shapes are well defined and can be accurately analyzed (Rodriguez et al., 2003; Rodriguez et al., 2006). Once the confocal images were deconvolved they were analyzed with NeuronStudio to examine global and local morphometric characteristics of dendrites and spines such as dendritic branching topology, dendritic varicosities, spine shape (stubby, mushroom, and thin), length and density. This software allows for automated digitization and reconstructions of 3-dimensional neuronal morphology from multiple confocal stacks on a spatial scale and averts the subjective errors encountered during manual tracing.

Electrophysiological recordings

The animals were sacrificed by decapitation and the brain specimens were quickly removed. The hippocampus was hemisected and placed into ice-cold oxygenated artificial cerebrospinal fluid (ACSF) for 1 min. The composition of ACSF was: 10 mM D-glucose, 124 mM NaCl, 1.25 mM NaH_2PO_4, 26 mM $NaHCO_3$, 4.9 mM KCL, 1 mM $CaCl_2$ and 4 mM $MgCl_2$; and was saturated with 95% O_2 + 5% CO_2. Immediately thereafter, both hippocampi were dissected and sliced using a tissue chopper (350 μm). Slices were transferred to a recording chamber and perfused continuously with oxygenated-ACSF. An automatic temperature control unit allowed a water bath to be maintained at 32°C, thus allowing the perfusing ACSF to be warmed to this temperature. Slices were perfused at a

rate of 1 ml/min and humidified with 95% O_2 + 5% CO_2 gas during the length of the experiment.

For extracellular recordings, Schaffer collateral projections from the CA3 region were stimulated with a monopolar stainless steel electrode (100 μm diameter) for activation of the CA1 neurons. A recording borosilicate glass electrode, filled with 3M NaCl with 1–2 M resistance was placed in the CA1 region to record field excitatory postsynaptic potentials (fEPSP). The recording electrode was placed within 150–200 μm of the stimulating electrode. Constant current pulses (150μs, 20–30 μA) were delivered using a stimulus isolator unit (A310 Accupulser, World Precision Instruments) and evoked fEPSPs were recorded with an amplifier (A-M Systems) and monitored on a digital oscilloscope. Responses were elicited every 1 min and digitalized, stored and analyzed using an Apple Macintosh computer and custom built software based on Lab-View 5.1 software by National Instruments.

Results

The effect of carvedilol on Aβ oligomerization by PICUP analysis

Structural analysis suggested that carvedilol might be able to bind to Aβ and therefore preventing Aβ to aggregate into oligomeric fibrils (Howlett et al., 1999). In *in vitro* studies using the photo-induced cross-linking of unmodified proteins (PICUP) technique, we explored the impact of carvedilol on initial peptide-to-peptide interactions that are necessary for spontaneous oligomerization of Aβ peptides (Vollers et al., 2005). In the absence of cross-linking, only $Aβ_{1–42}$ monomers and trimers and $Aβ_{1–40}$ monomers were revealed on the SDS-PAGE gel (Figure 1a, lane 1, left panel for $Aβ_{1–42}$, middle panel for $Aβ_{1–40}$; the $Aβ_{1–42}$ trimer band is an SDS-induced artifact). Using cross-linking to stabilize Aβ peptide-to-peptide interactions, we confirmed that Aβ peptides spontaneously aggregate into multimeric conformers; $Aβ_{1–42}$ formed a mixture of monomers and oligomers of orders 2–6, whereas $Aβ_{1–40}$ formed a mixture of monomers and oligomers of orders 2–4 (Figure 1a, lane 2, left panel for $Aβ_{1–42}$ and middle panel for $Aβ_{1–40}$). We found that $Aβ_{1–42}$ oligomerization was blocked almost completely by carvedilol (Figure 1a, left panel, lane 3: equal molar concentrations of carvedilol and $Aβ_{1–42}$ peptide). Carvedilol also interfered with oligomerization of $Aβ_{1–40}$ in a dose-dependent manner. Incubtion of $Aβ_{1–40}$ with carvedilol at equimolar concentrations completely abolished the formation of aggregated $Aβ_{1–40}$ tetramers species and significantly reduced the generation of $Aβ_{1–40}$ trimers and dimers species (Figure 1a, middle panel, lane 3). In the presence of a tenfold excess of carvedilol, the formation of $Aβ_{1–40}$ trimers was completely blocked and the amount of $Aβ_{1–40}$ dimers was further reduced (Figure 1a, middle panel, lane 4). In a control study, we confirmed that carvedilol did not interfere with the PICUP chemistry itself, as reflected by a similar distribution pattern of glutathione-S-transferase (GST) oligomers in the presence or absence of carvedilol (Figure 1a, right panel).

The effect of carvedilol on Aβ secondary structure dynamics by CD

Using circular dichroism (CD) spectroscopy, we examined the effects of carvedilol on the secondary structure of Aβ. Self-assembly of Aβ is characterized by a conformational transition from random coil to α-helix to β-sheet (Kirkitadze et al., 2001). Normal spontaneous aggregations of $Aβ_{1–40}$ and $Aβ_{1–42}$ peptides produce a shift in minimum molar ellipticity from ~195 nm to ~215–220 nm that reflects the transition from random coil to β-helix/β-sheet during the first three days of incubation (Figure 1b). We found that carvedilol inhibited the conformational transition of Aβ peptides from random coil to α-helix and β-sheet conformers in a dose-dependent manner (Figure 1b).

The effect of carvedilol on Aβ assembly morphology by EM

We next applied an electron microscopy (EM) methodology to examine the structural morphology of the $A\beta_{1–42}$ and $A\beta_{1–40}$ assemblies in the presence and absence of carvedilol. Consistent with PICUP and CD studies, carvedilol strongly attenuated fibril assembly for both $A\beta_{1–42}$ and $A\beta_{1–40}$ peptides. Compared to control $A\beta_{1–40}$ fibrils generated in the absence of carvedilol, we found that co-incubation of $A\beta_{1–40}$ with equimolar concentrations of carvedilol markedly reduced the number of fibrils formed and that fibrils generated in the presence of carvedilol were quantitatively thinner (4 nm versus 8 nm) (Figure 1c, bottom panel) and shorter and characterized by amorphous aggregates (Figure 2c, bottom panel). The impact of carvedilol on $A\beta_{1–42}$ assembly were similar to those on $A\beta_{1–40}$ peptide; co-treatment of $A\beta_{1–42}$ with carvedilol significantly reduced both the number and the length of fibrils, and increased the frequency of amorphous aggregates (Figure 2c, top panel).

Collectively, our *in vitro* studies suggest that carvedilol inhibits aggregations of Aβ peptides into structurally ordered neuropathological Aβ conformers, in part by interfering with Aβ peptide protein-protein interactions. Based on this observation we tested the physiological relevance of carvedilol in AD by exploring the role of carvedilol in cognitive function and neuropathology using independent TgCRND8 (see below) and Tg2576 (Supplementary Data) AD mouse models.

Carvedilol is well tolerated and is detected in the mouse brain following oral administration

At 3 months of age, TgCRND8 mice start to develop amyloid plaque, and at 5–6 months of age, TgCRND8 mice present AD-type neuropathology and cognitive deficits similar to that seen in human AD, as well as altered synaptic function and neuroplasticity (Chishti et al., 2001; Jolas et al., 2002). Starting at eight weeks of age, approximately four weeks before the onset of the AD-type amyloid accumulation, TgCRND8 mice were given 1.5 mg/kg/day carvedilol, which is equivalent to 7.5 mg per day in human. This dose is 2–3 times lower than the prescribed dosage for treating cardiovascular dysfunction in human.

Consistent with a previous observation that carvedilol easily crosses the blood-brain barrier (Bart et al., 2005), we found accumulations of carvedilol in the brain after 5 months of treatment (Figure 2a). No detectable levels of carvedilol were obtained in the brain tissues of strain-, age- and gender-matched water-treated control mice (data not shown). Consistent with evidence that carvedilol is highly tolerable, we found that 5 months of carvedilol treatment delivered through drinking water was well tolerated by TgCRND8 mice without any adverse effects as reflected by their stable body weight and unaltered blood pressure and heart rate (Figure 2b and 2c). We also observed a reduced mortality rate in the carvedilol treated TgCRND8 mice compared to the water treated controls (Figure 2d). In an independent study, we found that 5 months of carvedilol treatment was also well tolerated in the Tg2576 mouse model of AD (Supplementary Figure 1a).

Carvedilol treatment improves cognitive function in AD mice

Based on the observation that carvedilol is bioavailable in the brain and well-tolerated, we used the Morris water maze (MWM) test to explore the functional role of carvedilol treatment in attenuating cognitive deterioration. We found that 5 months of carvedilol treatment led to significant improvements in behavioral cognitive functions of TgCRND8 mice relative to water-treated control TgCRND8 mice ($p = 0.015$ for treatment effect, Figure 3a, left panel). More importantly, the carvedilol-treated group showed significantly improved spatial memory retention in the MWM probe trial after 24 hours ($P < 0.05$) (Figure 3a, right panel). In parallel control studies, we confirmed that both groups performed equally well in a visible trial, excluding the possibility that drug treatment might affect non-

spatial parameters, such as sensorimotor performance and motivation (data not shown). We continued to assess the effect of carvedilol on cognitive behavioral functions in AD mouse models using an independent, novel object recognition test (Ennaceur and Delacour, 1988). We found a tendency for carvedilol-treated TgCRND8 mice to spend more time exploring the novel object in the short-term (1-hour) memory test, compared to control, non-treated TgCRND8 mice, but the difference was not statistically significant (carvedilol-treated mice, 68.2 ± 3.7 % versus control mice 62.4 ± 3.1 %, $p = 0.26$; Figure 3b). However, when animals were assessed for long-term memory consolidation (24-hour test), we found that carvedilol-treated TgCRND8 mice performed significantly better and spent significantly more time exploring the novel object compared to control, non-treated TgCRND8 mice (65.7 ± 2.6 % vs. 51.7 ± 2.8 %, $p < 0.05$; Figure 3b). In control studies, we found that carvedilol treatment did not influence cognitive function in wild type animals (Supplementary Figure 2a).

Consistent with our observation in the TgCRD8 AD mouse model, we found that 5 months of carvedilol treatment also significantly attenuated cognitive deterioration in Tg2576 mice, as evaluated by the MWM test and the novel object recognition test (Supplementary Figure 1b and 1c).

Collectively, our observation from two independent AD mouse models using two independent cognitive behavioral tests demonstrate that carvedilol benefits spatial memory as well as general memory function in AD-type mice by interfering with AD-type Aβ-mediated brain injury.

Carvedilol treatment reduces oligomeric Aβ and improves basal synaptic transmission in the brains of AD mice

Because cognitive deterioration in AD mouse models like the TgCRND8 and Tg2576 mice correlated with the accumulation of soluble oligomeric Aβ, we then evaluated brain oligomeric Aβ content by quantitative ELISA and Western blot analysis, as previously described (Wang et al., 2008). Both assays revealed a significant reduction in soluble oligomeric Aβ content in the carvedilol-treated mouse brain (Figure 3c, left panel for ELISA, $p < 0.01$; right panel for Western blot, $p < 0.05$), The reduced oligomeric Aβ in the brain coincided with improvements in other AD-associated neuropathological markers, such as plaque burden in the brain (Figure 3d) and reduced total $A\beta_{1–42}$ (91.8±16.6 ng/mg protein in control group *vs* 142.5±13.6 ng/mg protein in carvedilol treated group, *$p<0.05$) and $A\beta_{1–40}$ levels (48.2±15.5 ng/mg protein in control group *vs* 83.1±9.9 ng/mg protein in carvedilol treated group, *$p<0.05$). We found that chronic carvedilol treatment did not affect the level of total APP transgene expression in the brain of TgCRND8 mice (Supplementary Figure 2b).

Consistent with these observations in TgCRND8 mice, we also found significant attenuation of total Aβ content, as well as oligomeric Aβ, in the brains of Tg2576 mice treated with carvedilol for 5 months (Supplementary Figure 1d and 1e).

Synaptic transmission and plasticity are essential to cognitive function. Oligomeric Aβ was indicated to play important role in the early pathogenesis and synapse loss in AD (Lambert et al., 1998; Walsh et al., 2002; Gylys et al., 2003; Coleman et al., 2004; Rowan et al., 2005; Shankar et al., 2008). We hypothesized that carvedilol treatment would reduce oligomeric Aβ, and therefore might have a beneficial impact on neuronal transmission by attenuating oligomeric-Aβ-mediated synaptic toxicity, especially in lieu of the fact that carvedilol does not affect cognitive function in wild type mice. We analyzed the hippocampal slices from carvedilol-treated TgCRND8 mice, and found that the strength of the basal synaptic transmission was significantly improved in carvedilol-treated TgCRND8 mice relative to

water-treated control mice, as measured by the field excitatory postsynaptic potentials (fEPSP) slope. The maximum fEPSP slope was 5.2 ± 0.36 for the water-treated control group (n = 7 slices) and 8.48 ± 1.04 for the carvedilol-treated group (n = 10 slices, $p < 0.001$; Figure 3e), suggesting that chronic carvedilol treatment could reestablish the strength of basal synaptic transmission in the CA1 region of hippocampal slices following stimulation of the Schaffer collateral projections from the CA3 region. Thus, our study supports the role of carvedilol in reducing Aβ oligomerization and protecting the integrity of neuronal transmission in TgCRND8 mice.

Carvedilol treatment retains the amount of “learning” thin spines

Dendritic spines are major sites of synaptic transmission, and their density and proper structure are essential for synaptic plasticity. Normally, about 65% of all spines in the mature brain are comprised of thin dendritic spines (Peters and Kaiserman-Abramof, 1970; Harris et al., 1992). Thin dendritic spines are morphologically less stable than other dendritic spines (e.g., stubby spines, mushroom shaped spines), but they are considered important for learning processes. We found that cognitive deterioration in TgCRND8 mice was associated with a reduced proportion of thin dendritic spines (54.1 ± 4.0%) compared to the normal ~65% observed in wild type mice. In contrast, carvedilol treatment retained the percentage of thin spines almost to wild type levels (62.2 ± 1.6 %). This change correlated with a significant reduction in the amounts of stubby spines (30.9 ± 3.3 % in control water-treated vs. 23.1 ± 0.8 % in carvedilol-treated mice; Figure 3f, right panel, thin spine/stubby spine ratio, $p < 0.01$). No difference was observed in the percentage of the mature mushroom type of dendritic spines, nor in spine density, in the brain of carvedilol-treated vs. non-treated TgCRND8 mice (control, 2.43 ± 0.68 spines/m of dendrites vs. carvedilol, 2.43 ± 0.55 spines/m of dendrites). Collectively, our evidence from *in vitro* Aβ assembly studies and *in vivo* preclinical studies in AD mouse models demonstrates the efficacy of carvedilol treatment to mitigate AD-type cognitive deterioration, in part by interfering with oligomeric Aβ-mediated neurotoxicity, leading to the preservation of key anatomic structures necessary for normal synaptic function.

Discussion

Oligomeric Aβ has been shown to impair synapse generation and synaptic plasticity (Terry et al., 1991; Lambert et al., 1998; Selkoe, 2002; Walsh et al., 2002; Scheff and Price, 2003; Gylys et al., 2003; Lacor et al., 2004; Coleman et al., 2004; Jacobsen et al., 2006; Shankar et al., 2007; Shankar et al., 2008). In this study, we showed that carvedilol, a widely prescribed, highly tolerated β-adrenergic receptor blocker, can significantly attenuate Aβ peptide fibrillation and oligomerization by several different biophysical measures. PICUP analysis revealed that carvedilol interferes with early stage Aβ dimer, trimer, and tetramer ($Aβ_{1–40}$) or pentamer and hexamer ($Aβ_{1–42}$) formation. Independent CD spectroscopy and EM studies confirmed that carvedilol effectively prevents the formation of ordered α-helix and β-sheet conformers or protofibrils. Moreover, chronic carvedilol treatment attenuated spatial memory deterioration, coincidental with a reduction in soluble oligomeric Aβ content in the brains of TgCRND8 and Tg2576 mice. Since carvedilol is highly bioavailable in the brain and is able to physically interact with Aβ peptides, it is very likely that carvedilol exerts its biological function by preventing Aβ fibrillation and oligomerization in the brain of AD mice.

Given the strong anti- Aβ fibrillation/oligomerization activity of carvedilol, it is possible that carvedilol interferes directly (or indirectly) with fibrillary and oligomeric Aβ formation and prevents its neurotoxic interactions at the dendritic spine and synapse level. Consistent with this hypothesis, cortical neurons obtained from carvedilol-treated TgCRND8 mice retained a higher proportion of thin spines, comparable to that found in wild type animals, whereas

untreated TgCRND8 mice had significantly fewer thin spines. Thin dendritic spines are considered to be responsible for learning and the maintenance of structural flexibility to accommodate key inputs, compared to the more stable mushroom spines (Kasai et al., 2003; Zuo et al., 2005; Holtmaat et al., 2005). Thus, carvedilol treatment leading to the preservation of dendritic thin spines might contribute to the maintenance of basal synaptic transmission, and hence improved cognitive function, as observed in carvedilol-treated TgCRND8 mice.

Evidence also shows that therapeutic efficacy of carvedilol for treating cardiovascular diseases is mediated, in part, through its antioxidant and anti-inflammatory activities (Dandona P et al., 2007; Hayashi et al., 2008). Exposure to carvedilol has also been shown to be neuroprotective (Savitz et al., 2000; Goyagi et al., 2006; Hayashi et al., 2008) and associated with a slower rate of functional decline in AD (Rosenberg et al., 2008). Both oxidative stress and inflammation have been implicated in the pathogenesis of AD, thus it is possible that the previously described antioxidant and anti-inflammatory activity of carvedilol might contribute to its ability to interfere with AD-type cognitive deterioration in our transgenic mouse models.

Carvedilol is a non-selective adrenergic receptor antagonist. It was reported that the application of β-blockers could affect delayed memory in patients with cognitive impairment, while other studies showed that β-blockers did not have any negative effect on cognition(Perez-Stable et al., 1992; Sabe r and Cain, 2003). Studies using experimental models have shown that spatial memory performance worsened following a combination of serotonin depletion and antagonism of β-adrenergic receptors, while either depletion of serotonin or antagonism of β-adrenergic receptors alone was shown to cause no impairments (Kenton et al., 2007; Gliebus and Lippa, 2007). In our study, the application of carvedilol alone at doses 2–3 times lower than the equivalent dosage prescribed in humans to treat cardiovascular dysfunction may have been low enough, so as not to induce any adverse effect in cognitive function. However, future studies exploring the mechanisms underlying carvedilol absorption and eventually carvedilol-Aβ pharmacokinetics and pharmacodynamics in the brain, in addition to the extent to which brain beta receptors are being blocked, will further clarify the biochemical and pharmacological role of carvedilol in preventing Aβ-mediated responses.

Collectively, evidence from our *in vitro* studies revealing that carvedilol interferes with Aβ aggregation mechanisms, and from our preclinical studies demonstrating the efficacy of carvedilol treatment to mitigate AD-type amyloid neuropathology and cognitive dysfunction in AD mouse models, supports the continued development of carvedilol for the treatment (and/or prevention) of AD dementia.

Supplementary Material

Refer to Web version on PubMed Central for supplementary material.

Acknowledgments

This work is supported by NIH UO1 AG29310 (GMP) and funding provided by Altschul Foundation.

References

Bart J, Dijkers ECF, Wegman TD, de Vries EGE, van der Graaf WTA, Groen HJM, Vaalburg W, Willemsen ATM, Hendrikse NH. New positron emission tomography tracer [^{11}C]carvedilol reveals P-glycoprotein modulation kinetics. Br J Pharmacol. 2005; 145:1045–1051. [PubMed: 15951832]

Bevins RA, Besheer J. Object recognition in rats and mice: a one-trial non-matching-to-sample learning task to study 'recognition memory'. Nat Protocols. 2006; 1:1306–1311.

Bitan G, Lomakin A, Teplow DB. Amyloid beta -Protein Oligomerization. Prenucleation interactions revealed by photo-induced cross-linking of unmodified proteins. J Biol Chem. 2001; 276:35176–35184. [PubMed: 11441003]

Chishti MA, Yang DS, Janus C, Phinney AL, Horne P, Pearson J, Strome R, Zuker N, Loukides J, French J, Turner S, Lozza G, Grilli M, Kunicki S, Morissette C, Paquette J, Gervais F, Bergeron C, Fraser PE, Carlson GA, George-Hyslop PS, Westaway D. Early-onset amyloid deposition and cognitive deficits in transgenic mice expressing a double mutant form of amyloid precursor protein 695. J Biol Chem. 2001; 276:21562–21570. [PubMed: 11279122]

Cleary JP, Walsh DM, Hofmeister JJ, Shankar GM, Kuskowski MA, Selkoe DJ, Ashe KH. Natural oligomers of the amyloid-[beta] protein specifically disrupt cognitive function. Nat Neurosci. 2005; 8:79–84. [PubMed: 15608634]

Coleman P, Federoff H, Kurlan R. A focus on the synapse for neuroprotection in Alzheimer disease and other dementias. Neurology. 2004; 63:1155–1162. [PubMed: 15477531]

Dandona P, Ghanim H, Brooks DP. Antioxidant activity of carvedilol in cardiovascular disease. J Hypertens. 2007; 25:731–41. [PubMed: 17351362]

Duan H, Wearne SL, Morrison JH, Hof PR. Quantitative analysis of the dendritic morphology of corticocortical projection neurons in the macaque monkey association cortex. Neuroscience. 2002; 114:349–359. [PubMed: 12204204]

Duan H, Wearne SL, Rocher AB, Macedo A, Morrison JH, Hof PR. Age-related Dendritic and Spine Changes in Corticocortically Projecting Neurons in Macaque Monkeys. Cereb Cortex. 2003; 13:950–961. [PubMed: 12902394]

Ennaceur A, Delacour J. A new one-trial test for neurobiological studies of memory in rats. 1: Behavioral data. Behav Brain Res. 1988; 31:47–59. [PubMed: 3228475]

Gliebus G, Lippa CF. The Influence of β-Blockers on Delayed Memory Function in People With Cognitive Impairment. American Journal of Alzheimer's Disease and Other Dementias. 2007; 22:57–61. [PubMed: 17534003]

Goyagi T, Kimura T, Nishikawa T, Tobe Y, Masaki Y. β-Adrenoreceptor Antagonists Attenuate Brain Injury After Transient Focal Ischemia in Rats. Anesth Analg. 2006; 103:658–66. [PubMed: 16931677]

Gylys KH, Fein JA, Tan AM, Cole GM. Apolipoprotein E enhances uptake of soluble but not aggregated amyloid-beta protein into synaptic terminals. J Neurochem. 2003; 84:1442–1451. [PubMed: 12614344]

Hao J, Rapp PR, Leffler AE, Leffler SR, Janssen WGM, Lou W, McKay H, Roberts JA, Wearne SL, Hof PR, Morrison JH. Estrogen Alters Spine Number and Morphology in Prefrontal Cortex of Aged Female Rhesus Monkeys. J Neurosci. 2006; 26:2571–2578. [PubMed: 16510735]

Harris KM, Jensen FE, Tsao B. Three-dimensional structure of dendritic spines and synapses in rat hippocampus (CA1) at postnatal day 15 and adult ages: implications for the maturation of synaptic physiology and long-term potentiation. J Neurosci. 1992; 12:2685–2705. [PubMed: 1613552]

Hayashi T, Saitou Y, Nose K, Nishioka T, Ishii T, Uemura H. Efficacy of Carvedilol for Ischemia/Reperfusion-Induced Oxidative Renal Injury in Rats. Transplantation Proceedings. 2008; 40:2139–2141. [PubMed: 18790173]

Holtmaat AJ, Trachtenberg JT, Wilbrecht L, Shepherd GM, Zhang X, Knott GW, Svoboda K. Transient and persistent dendritic spines in the neocortex in vivo. Neuron. 2005; 45:279–291. [PubMed: 15664179]

Howlett DR, George AR, Owen DE, Ward RV, Markwell RE. Common structural features determine the effectiveness of carvedilol, daunomycin and rolitetracycline as inhibitors of Alzheimer beta-amyloid fibril formation. Biochem J. 1999; 343:419–423. [PubMed: 10510309]

Hsiao K, Chapman P, Nilsen S, Eckman C, Harigaya Y, Younkin S, Yang F, Cole G. Correlative Memory Deficits, Abeta Elevation, and Amyloid Plaques in Transgenic Mice. Science. 1996; 274:99–103. [PubMed: 8810256]

Jacobsen JS, Wu CC, Redwine JM, Comery TA, Arias R, Bowlby M, Martone R, Morrison JH, Pangalos MN, Reinhart PH, Bloom FE. Early-onset behavioral and synaptic deficits in a mouse model of Alzheimer's disease. PNAS. 2006; 103:5161–5166. [PubMed: 16549764]

Jolas T, Zhang XS, Zhang Q, Wong G, Vecchio RD, Gold L, Priestley T. Long-Term Potentiation Is Increased in the CA1 Area of the Hippocampus of APPswe/ind CRND8 Mice. Neurobiology of Disease. 2002; 11:394–409. [PubMed: 12586549]

Kasai H, Matsuzaki M, Noguchi J, Yasumatsu N, Nakahara H. Structure-stability-function relationships of dendritic spines. Trends Neurosci. 2003; 26:360–368. [PubMed: 12850432]

Kenton L, Boon F, Cain DP. Combined but not Individual Administration of [beta]-Adrenergic and Serotonergic Antagonists Impairs Water Maze Acquisition in the Rat. Neuropsychopharmacology. 2007; 33:1298–1311. [PubMed: 17653108]

Kirkitadze MD, Condron MM, Teplow DB. Identification and characterization of key kinetic intermediates in amyloid β-protein fibrillogenesis. Journal of Molecular Biology. 2001; 312:1103–1119. [PubMed: 11580253]

Klein WL. Aβ toxicity in Alzheimer's disease: globular oligomers (ADDLs) as new vaccine and drug targets. Neurochemistry International. 2002; 41:345–352. [PubMed: 12176077]

Klyubin I, Walsh DM, Lemere CA, Cullen WK, Shankar GM, Betts V, Spooner ET, Jiang LY, Anwyl R, Selkoe DJ, Rowan MJ. Amyloid beta protein immunotherapy neutralizes A beta oligomers that disrupt synaptic plasticity in vivo. Nature Medicine. 2005; 11:556–561.

Kotilinek LA, Bacskai B, Westerman M, Kawarabayashi T, Younkin L, Hyman BT, Younkin S, Ashe KH. Reversible memory loss in a mouse transgenic model of Alzheimer's disease. J Neurosci. 2002; 22:6331–6335. [PubMed: 12151510]

Lacor PN, Buniel MC, Chang L, Fernandez SJ, Gong Y, Viola KL, Lambert MP, Velasco PT, Bigio EH, Finch CE, Krafft GA, Klein WL. Synaptic Targeting by Alzheimer's-Related Amyloid β Oligomers. J Neurosci. 2004; 24:10191–10200. [PubMed: 15537891]

Lambert MP, Barlow AK, Chromy BA, Edwards C, Freed R, Liosatos M, Morgan TE, Rozovsky I, Trommer B, Viola KL, Wals P, Zhang C, Finch CE, Krafft GA, Klein WL. Diffusible, nonfibrillar ligands derived from Abeta 1–42 are potent central nervous system neurotoxins. PNAS. 1998; 95:6448–6453. [PubMed: 9600986]

Lesne S, Koh MT, Kotilinek L, Kayed R, Glabe CG, Yang A, Gallagher M, Ashe KH. A specific amyloid-beta protein assembly in the brain impairs memory. Nature. 2006; 440:352–357. [PubMed: 16541076]

Lyketsos CG, Reichman WE, Paul Kershaw, Young Zhu. Long-Term Outcomes of Galantamine Treatment in Patients With Alzheimer Disease. Am J Geriatr Psychiatry. 2004; 12:473–482. [PubMed: 15353385]

McLaurin J, Kierstead ME, Brown ME, Hawkes CA, Lambermon MHL, Phinney AL, Darabie AA, Cousins JE, French JE, Lan MF, Chen F, Wong SSN, Mount HTJ, Fraser PE, Westaway D, George-Hyslop PS. Cyclohexanehexol inhibitors of Aβ aggregation prevent and reverse Alzheimer phenotype in a mouse model. Nat Med. 2006; 12:801–808. [PubMed: 16767098]

Morris R. Developments of a water-maze procedure for studying spatial-learning in the rat. Journal of Neuroscience Methods. 1984; 11:47–60. [PubMed: 6471907]

Packer M, Bristow MR, Cohn JN, Colucci WS, Fowler MB, Gilbert EM, Shusterman NH. The U.S. Carvedilol Heart Failure Study Group. The Effect of Carvedilol on Morbidity and Mortality in Patients with Chronic Heart Failure. N Engl J Med. 1996; 334:1349–1355. [PubMed: 8614419]

Perez-Stable EJ, Coates TJ, Halliday R, Gardiner PS, Hauck WW. The effects of mild diastolic hypertension on the results of tests of cognitive function in adults 22 to 59 years of age. J Gen Intern Med. 1992; 7:19–25. [PubMed: 1548544]

Peters A, Kaiserman-Abramof IR. The small pyramidal neuron of the rat cerebral cortex. The perikaryon, dendrites and spines. Am J Anat. 1970; 127:321–355. [PubMed: 4985058]

Radley JJ, Rocher AB, Miller M, Janssen WGM, Liston C, Hof PR, McEwen BS, Morrison JH. Repeated Stress Induces Dendritic Spine Loss in the Rat Medial Prefrontal Cortex. Cereb Cortex. 2006; 16:313–320. [PubMed: 15901656]

Rodriguez A, Ehlenberger D, Kelliher K, Einstein M, Henderson SC, Morrison JH, Hof PR, Wearne SL. Automated reconstruction of three-dimensional neuronal morphology from laser scanning microscopy images. Methods. 2003; 30:94–105. [PubMed: 12695107]

Rodriguez A, Ehlenberger DB, Hof PR, Wearne SL. Rayburst sampling, an algorithm for automated three-dimensional shape analysis from laser scanning microscopy images. Nat Protocols. 2006; 1:2152–2161.

Rosenberg PB, Mielke MM, Tschanz J, Cook L, Corcoran C, Hayden KM, Norton M, Rabins PV, Green RC, Welsh-Bohmer KA, Breitner JC, Munger R, Lyketsos CG. Effects of cardiovascular medications on rate of functional decline in Alzheimer disease. Am J Geriatr Psychiatry. 2008; 16:883–892. [PubMed: 18978249]

Rowan MJ, Klyubin I, Wang Q, Anwyl R. Synaptic plasticity disruption by amyloid beta protein: modulation by potential Alzheimer's disease modifying therapies. Biochem Soc Trans. 2005; 33:563–567. [PubMed: 16042545]

Saber AJ, Cain DP. Combined beta-adrenergic and cholinergic antagonism produces behavioral and cognitive impairments in the water maze: implications for Alzheimer disease and pharmacotherapy with beta-adrenergic antagonists. Neuropsychopharmacology. 2003; 28:1247–1256. [PubMed: 12700678]

Savitz SI, Erhardt JA, Anthony JV, Gupta G, Li X, Barone FC, Rosenbaum DM. The Novel β-Blocker, Carvedilol, Provides Neuroprotection in Transient Focal Stroke. J Cereb Blood Flow Metab. 2000; 20:1197–1204. [PubMed: 10950380]

Scheff SW, Price DA. Synaptic pathology in Alzheimer's disease: a review of ultrastructural studies. Neurobiology of Aging. 2003; 24:1029–1046. [PubMed: 14643375]

Seabrook TJ, Thomas K, Jiang L, Bloom J, Spooner E, Maier M, Bitan G, Lemere CA. Dendrimeric A[beta]1–15 is an effective immunogen in wildtype and APP-tg mice. Neurobiology of Aging. 2007; 28:813–823. [PubMed: 16725229]

Selkoe DJ. Alzheimer's disease is a synaptic failure. Science. 2002; 298:789–791. [PubMed: 12399581]

Shankar GM, Bloodgood BL, Townsend M, Walsh DM, Selkoe DJ, Sabatini BL. Natural Oligomers of the Alzheimer Amyloid-β Protein Induce Reversible Synapse Loss by Modulating an NMDA-Type Glutamate Receptor-Dependent Signaling Pathway. J Neurosci. 2007; 27:2866–2875. [PubMed: 17360908]

Shankar GM, Li S, Mehta TH, Garcia-Munoz A, Shepardson NE, Smith I, Brett FM, Farrell MA, Rowan MJ, Lemere CA, Regan CM, Walsh DM, Sabatini BL, Selkoe DJ. Amyloid-β protein dimers isolated directly from Alzheimer's brains impair synaptic plasticity and memory. Nat Med. 2008; 14:837–842. [PubMed: 18568035]

Sholl A, Uttley AM. Pattern discrimination and the visual cortex. Nature. 2009; 171:387–388. [PubMed: 13036904]

Terry RD, Masliah E, Salmon DP, Butters N, Deteresa R, Hill R, Hansen LA, Katzman R. Physical Basis of Cognitive Alterations in Alzheimers-Disease - Synapse Loss Is the Major Correlate of Cognitive Impairment. Annals of Neurology. 1991; 30:572–580. [PubMed: 1789684]

Vollers SS, Teplow DB, Bitan G. Determination of Peptide oligomerization state using rapid photochemical crosslinking. Methods Mol Biol. 2005; 299:11–18. [PubMed: 15980592]

Walsh DM, Klyubin I, Fadeeva JV, Cullen WK, Anwyl R, Wolfe MS, Rowan MJ, Selkoe DJ. Naturally secreted oligomers of amyloid [beta] protein potently inhibit hippocampal long-term potentiation in vivo. Nature. 2002; 416:535–539. [PubMed: 11932745]

Wang J, Ho L, Chen L, Zhao Z, Zhao W, Qian X, Humala N, Seror I, Bartholomew S, Rosendorff C, Pasinetti GM. Valsartan lowers brain beta-amyloid protein levels and improves spatial learning in a mouse model of Alzheimer disease. J Clin Invest. 2007; 117:3393–3402. [PubMed: 17965777]

Wang J, Ho L, Qin W, Rocher AB, Seror I, Humala N, Maniar K, Dolios G, Wang R, Hof PR, Pasinetti GM. Caloric restriction attenuates beta-amyloid neuropathology in a mouse model of Alzheimer's disease. FASEB J. 2005; 19:659–661. [PubMed: 15650008]

Wang J, Ho L, Zhao W, Ono K, Rosensweig C, Chen L, Humala N, Teplow DB, Pasinetti GM. Grape-derived polyphenolics prevent Abeta oligomerization and attenuate cognitive deterioration in a mouse model of Alzheimer's disease. J Neurosci. 2008; 28:6388–6392. [PubMed: 18562609]

Zhao W, Wang J, Ho L, Ono K, Teplow DB, Pasinetti GM. Identification of Antihypertensive Drugs Which Inhibit Amyloid-beta Protein Oligomerization. J Alzheimers Dis. 2009; 16:49–57. [PubMed: 19158421]

Zuo Y, Lin A, Chang P, Gan WB. Development of long-term dendritic spine stability in diverse regions of cerebral cortex. Neuron. 2005; 46:181–189. [PubMed: 15848798]

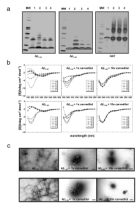

Figure 1. Carvedilol attenuates aggregation of Aβ peptides *in vitro*

(a) SDS-PAGE of $A\beta_{1–42}$ and $A\beta_{1–40}$ in the presence or absence of carvedilol following PICUP. $A\beta_{1–42}$ (left panel), $A\beta_{1–40}$ (middle panel), and glutathione S-transferase (GST) control (right panel) were cross-linked in the presence or absence of carvedilol and the bands in subsequent SDS gels were visualized using silver staining. In all three panels: MW, molecular weight; lanes 1, non-cross-linked $A\beta_{1–42}$, $A\beta_{1–40}$, or GST control; lanes 2, aggregated $A\beta_{1–42}$, $A\beta_{1–40}$, or GST, lanes 3 and 4, $A\beta_{1–42}$, $A\beta_{1–40}$, or GST aggregated in the presence of an equimolar concentration (lane 3) or 10× molar excess (lane 4) of carvedilol. The $A\beta_{1–42}$ trimer band (middle panel) has been shown to be an SDS-induced artifact. (b) Circular dichroism spectroscopy assessment of Aβ peptide secondary structure dynamics. $A\beta_{1–42}$ (top panel) and $A\beta_{1–40}$ (bottom panel) were incubated at 37 °C for 7 days alone in 10 mM phosphate, pH 7.4 (left panel), or in the presence of an equimolar concentration (middle panel) or 10× molar excess (right panel) of carvedilol. Spectra were acquired immediately at the start of the incubation period on day 0 and after 1, 2, 3, 6, and 7 days. The spectra presented at each time are representative of those obtained from each of 3 independent experiments. (c) Electron microscopy assessment of Aβ fibril morphology. As indicated, synthetic $A\beta_{1–42}$ (Figure 1c, top panel) or $A\beta_{1–40}$ (Figure 1c, bottom panel) incubated at 37 °C for 7 days either alone (left panel) or in the presence of an equimolar concentration (middle panel) or 10× molar excess to (right panel) of carvedilol. Scale bars indicate 100 nm.

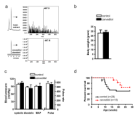

Figure 2. Carvedilol is bioavailable in the brain and Chronic carvedilol treatment is well tolerated

(a) Liquid chromatography (LC) separation and collected in-line electrospray ionization (ESI) + mass spectroscopy (MS) spectra of carvedilol from mouse brain extract (top panels) and carvedilol standard (bottom panels). (b)Measurements of body weight and (c) measurements of systolic, diastolic, mean arterial blood pressure (MAP), and pulse rate after 5 months of carvedilol treatment. (d) Chronic carvedilol treatment improves survival in TgCRND8 mice.

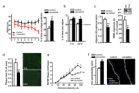

Figure 3. Chronic carvedilol treatment attenuates cognitive deterioration and improves neuroplasticity in the TgCRND8 mouse model of AD

(a) The influence of chronic carvedilol treatment on Aβ-related spatial memory in TgCRND8 mice vs. untreated control mice in the Morris water maze test. Hidden platform acquisition (left panel) latency score represents the time taken to escape to the platform from the water (two-way RM ANOVA; carvedilol vs. control group: $F_{1,112} = 7.26$; $p = 0.016$ for carvedilol-treatment, $F_{7,112} = 0.79$; $p = 0.601$ for time and $F_{7,112} = 1.23$; $p = 0.291$ for interaction). Probe trial (right panel): percent of time in quadrant is calculated as the ratio of time spent in the target quadrant area relative to the time spent in the rest of the pool; *, $p < 0.05$ (2-tailed student t-test). (b) Novel object recognition test of short-term working memory (1 hour) and long-term memory (24 hours) in TgCRND8 mice; *, $p < 0.05$ (2-tailed student t-test). (c) Quantification of oligomeric Aβ in the brains of water-treated control and carvedilol-treated mice by ELISA measurements (left panel) and western blot analysis (right panel). (c) Inset, representative Western blot of high molecular weight (HMW) soluble Aβ species (MW ~150 kDa). Values represent group mean ± SEM, N = 7–12 per group; *, $p < 0.05$ and **, $p < 0.01$, two-tailed Student's *t* test. (d) Plaque burden in the brains of TgCRND8 mice treated with H2O (control) and carvedilol. Inset: representative photomicrograph of amyloid plaques in the brains of control (CTL) and carvedilol (Carv)-treated TgCRND8 mice visualized by thioflavin-S staining. (e) Effect of carvedilol on basal synaptic transmission in hippocampal slices from water control and chronically carvedilol-treated TgCRND8 mice. Input-output curves were derived from the CA1 region to evaluate basal synaptic transmission as measured by the fEPSP slope; **, $p < 0.01$ two-way ANOVA. (f) Chronic carvedilol treatment increased the number of thin spines and reduced the stubby spines in the basal dendrites of prefrontal cortical neurons in TgCRND8 mice (left panel). Representative photomicrograph of spine segment and reconstructed segment of spines obtained from frontal cortical neuron of control and carvedilol-treated TgCRND8 mice (right panel). Values represent group mean ± SEM, N = 4–5 mice per group; **, $p < 0.01$.